

PAPER • OPEN ACCESS

Effect of gas volume fraction on the vortex motion within the oil-gas multiphase pump

To cite this article: G T Shi *et al* 2018 *IOP Conf. Ser.: Earth Environ. Sci.* **163** 012002

View the [article online](#) for updates and enhancements.

Related content

- [Effect of gas volume fraction on vortex motion in hydraulic turbine](#)
G T Shi, Y Liu, K Luo et al.
- [Study on the distribution regularity of gas volume in multiphase pump](#)
G T Shi, K Luo, Z W Wang et al.
- [The two-phase flow analysis of helico-axial oil-gas multiphase pump for offshore oil fields](#)
S Y Li, J Zhang, X P Jiang et al.



IOP | ebooks™

Bringing you innovative digital publishing with leading voices to create your essential collection of books in STEM research.

Start exploring the collection - download the first chapter of every title for free.

Effect of gas volume fraction on the vortex motion within the oil-gas multiphase pump

G T Shi^{1,2}, Z W Wang¹, K Luo¹, Y Liu¹ and X P Jiang³

¹Department of Power Machinery, University of Xihua, Chengdu, China

²State Key Laboratory of Hydrosience and Engineering & Department of Thermal Engineering, Tsinghua University, Beijing, 100084, China

³School of Mechanical Electronic & Information Engineering, China University of Mining & Technology (Beijing), Beijing 100083, China

952813670@qq.com

Abstract. In order to research the regular pattern of the vortex within the oil-gas multiphase pump with the gas volume fraction changes, the standard K-epsilon turbulence model is selected, the gas-liquid two-phase flow field within the multiphase pump is calculated by the CFD software under the different gas volume fraction, the regular pattern of the vortex motion within the multiphase pump is analyzed under the different gas volume fraction. The results show that, from the impeller hub to the rim, the vortex in the guide vane is gradually become smaller, the vortex within the impeller is gradually obvious, and with the increase of the gas volume fraction, the flow separation, the backflow and the vortex phenomenon within the impeller and the guide vane are gradually increased. It is also found that the flow separation has a greater influence on the turbulent dissipation within the whole flow field, that is, the more serious the area of off flow, the greater the energy loss. The results provide an important theoretical basis for the optimal design of the structure of oil-gas multiphase pump.

1. Introduction

Vortex generation, development, change is a very complex physical process, the vortex distribution varies greatly with the gas volume fraction. In the oil-gas multiphase pump, due to high gas volume fraction, which leads to the vortex motion within the pump is more complex, often causes oil-gas multiphase pump gas plug and plug flow and so on, results in poor performance, cannot work normally.

At present, the research on the flow mechanism within the multiphase pump is mainly focused on the velocity distribution and the gas volume distribution, the main methods used are numerical and experimental research. Ji etc. ^[1] calculated the unsteady cavitation flow field of the three-dimensional torsional hydrofoil by using the local time averaging model, described the evolution of horseshoe vortex. Zhang Jinya etc. ^[2] taken the compressible gas and water as the medium, calculated the compressible flow field within the three-stage spiral axial-flow oil-gas multiphase pump, pointed out the pressure variation law of the whole flow field within the multiphase pump with the change of gas volume fraction. Yu Zhiyi



etc.^[3] based on the bubble flow hypothesis, carried out the unsteady numerical simulation of the blade type multiphase pump. Ma Xijin etc.^[4] by using numerical simulation method, detailed analyzed the influence of blade number on the internal flow of axial-flow oil-gas multiphase pump. In the literature ^[5~12], the performance of the pump is researched from the aspects of pressure fluctuation, axial clearance, mechanical seal and the angle of the guide vane outlet. In recent years, people in addition to do lots of numerical calculation of the flow field within the multiphase pump, the experimental research on the pump was also carried out. Li Wei etc.^[13] by doing the PIV measurement test of the internal flow field within the guide vane multiphase pump, analyzed the influence of the change of flow on the flow field within the multiphase pump. Zhang Jinya etc.^[14] by setting the buffer equalizer in the front of the oil-gas multiphase pump, researched the visualization of the gas-liquid two-phase flow field of the inlet section of the pump, plotted the curves of the bubble diameter of the inlet of the pump with the change of the gas volume fraction and the pump rotating speed. Yang etc.^[15] carried out the experimental studies on the high gas volume fraction of the multiphase pump inlet, pointed out that the leakage loss of synchronous rotor multiphase pump at high gas volume fraction increases sharply, and the efficiency drops faster. Based on the above study, this paper through the numerical calculation method, the standard K- ϵ turbulence model is selected, under the gas volume fraction from the flow line distribution and turbulence dissipation analyzed the vortex motion in the flow field within the oil-gas multiphase pump.

2. Research object

In this paper, we take independent research and development of spiral axial-flow oil-gas multiphase pump as the research object. According to the design parameters of the model, 3D modeling of whole flow field by UG, as shown in figure 1. The compression unit is level 5, the main design parameters are, design flow $Q_d = 100\text{m}^3 / \text{h}$, head $H = 85\text{m}$, design speed $n = 2950\text{r} / \text{min}$, motor power $P = 55\text{kW}$. Gas volume fraction $GLR = 0-73\%$ (The gas volume fraction is the ratio of the volume flow of the gas phase medium to the volume flow rate of the mixture), efficiency = 33%. Considering the calculation of time and computer performance, select 3 as the research object. The impeller and the guide vane hub by the cone design, the diameter of the rim is $d_2 = 230\text{mm}$, the number of leaves of the impeller $Z_1 = 4$, the number of the guide vane blade $Z_2 = 9$.



Figure 1. whole flow field structure of model

3. Numerical calculation method

3.1 control equations

In numerical calculation, relative to many turbulence models, the standard K-epsilon turbulence model has better stability and applicability, has been confirmed by a large number of engineering and scientific research. And the y^+ value of this article is distributed between 1-80, which satisfies the requirements of K-epsilon turbulence model for near-wall grid quality. Based on this, in this paper, the standard K-epsilon turbulence model is chosen as the control equation.

The standard K-epsilon turbulence model needs to solve the turbulent kinetic energy and its dissipation rate equation. The turbulent kinetic energy k and the dissipation rate ε equation are as follows,

$$\rho \frac{Dk}{Dt} = \frac{\partial}{\partial x_i} \left[\left(\mu + \frac{\mu_t}{\sigma_k} \right) \frac{\partial k}{\partial x_i} \right] + G_k + G_b - \rho \varepsilon - Y_M \quad (1)$$

$$\rho \frac{D\varepsilon}{Dt} = \frac{\partial}{\partial x_i} \left[\left(\mu + \frac{\mu_t}{\sigma_k} \right) \frac{\partial \varepsilon}{\partial x_i} \right] + C_{1z} \frac{\varepsilon}{k} (G_k + G_{3z} G_b) - C_{2z} \rho \frac{\varepsilon^2}{k} \quad (2)$$

In the above equation, G_k represents the turbulent kinetic energy caused by the average velocity gradient, G_b represents the turbulent kinetic caused by the buoyancy, Y_M is the effect of compressible

turbulence pulsation inflated on the whole dissipation rate. The turbulence viscosity, $\mu_t = \rho C_\mu \frac{k^2}{\varepsilon}$. The coefficients in the model take the values in the single-phase flow, $\sigma_k = 1.0$, $\sigma_\varepsilon = 1.314$, $C_\mu = 0.09$, each scheme adopts second order upwind.

3.2 Grid division

In this paper, ICEM is used to divide the fluid domain of the impeller and the guide vane into hexahedral structured grid. The results of the grid are shown in figure 2 and figure 3, verified by grid independence, the final selection of the calculated grid leaf surface y^+ is distributed between 1-80. The number of suction chamber cells is 85,534, the number of extruded cells is 692624, the number of impeller cells is 528,219, the number of guide vane cells is 461768.



Figure 2. Impeller Grid



Figure 3. Guide vane grid

3.3 Boundary condition setting

Spatial discretization of transient control equation based on finite volume method, the coupling of pressure and velocity uses the SIMPLEC algorithm. The steady calculation results are taken as the initial values for the unsteady calculation, to enhance the stability of the calculation and improve the convergence rate.

The total time of calculating takes 5 times of the impeller rotation cycle, due to the number of grids and multi-phase calculation, the result file is large, so only processing and analysis the last cycle calculation of the results file data. The time step takes the time required for the impeller to rotate 2° . The calculation domain uses mass flow imports, pressure out-let boundary conditions. The walls are free of slip boundary conditions. In multi-stage multiphase pump, impeller and adjacent guide vanes formed two levels of static and dynamic interference. In the calculation, the problem of coupling between rotating impeller and stationary part is solved by sliding grid technique, so as to achieve accurate simulation of two levels of

static and dynamic interference flow.

4. Analysis of the results

4.1 Streamline distribution

Figure 4 is the streamline distribution of the half rotation surface at each height of the leaves under the conditions of the pure water, we can find from the figure, at 0.1 span, there is a great deal of the flow separation at the inlet of the guide vane, covered with the whole guide vane flow field, there is also a backflow in the individual guide vanes, but there is no vortex in the impeller. At 0.5 span, the vortex is mainly concentrated at the exit position of the guide vane working faces, the vortex here consist essentially of backflow vortex, the appearance of this phenomenon is likely to lead to poor design of the guide vane airfoil. At 0.9 span, the number of vortex is significantly reduced, but the impeller imports began to flow off. It can be seen that the vortex is gradually reduced from the hub to the rim guide vane under the pure water flow, and the vortex gradually become obvious.

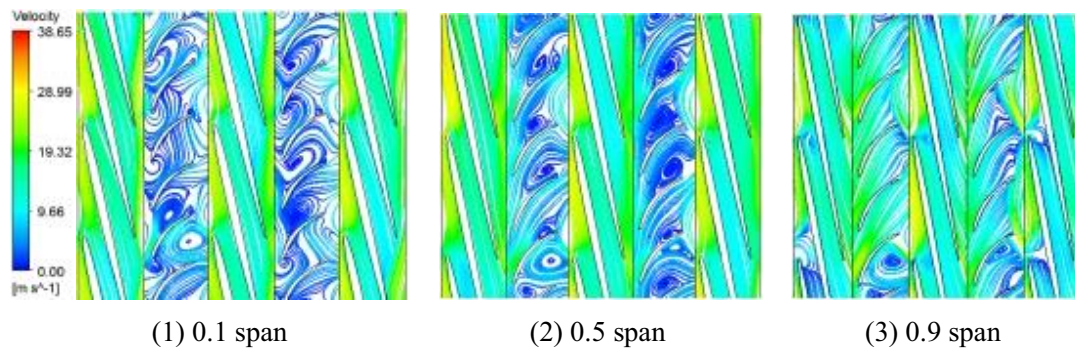


Figure 4. The streamline distribution of the half rotation surface at each span under the conditions of the pure water condition

Figure 5 is the streamline distribution of the half rotation surface at each span under the 20% gas volume fraction, as can be seen from the figure, at 0.1 span, the guide vane flow separation phenomenon is obvious. At 0.5 span, there is a significant vortex in the guide vane. At 0.9 span, there is a significant flow separation at the impeller inlet and the guide vane out-let. It can be seen that the flow separation phenomenon is more serious under the condition of gas-liquid two-phase than pure water.

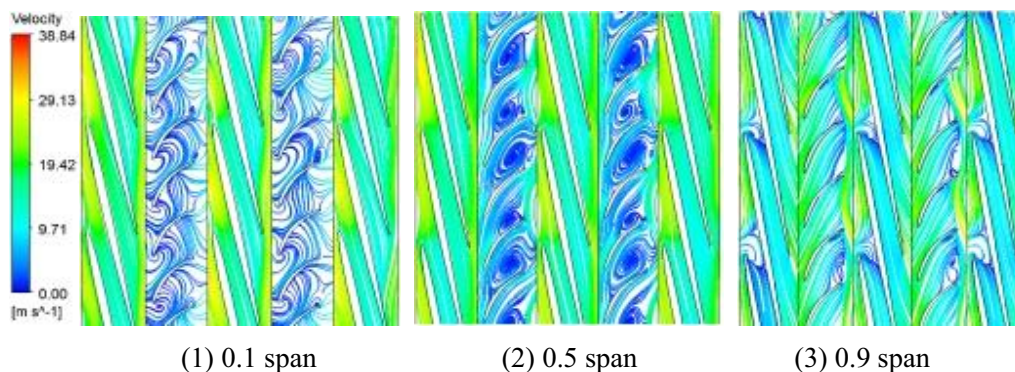


Figure 5. The streamline distribution of the half rotation surface at each span under the conditions of the 20% gas volume fraction

Figure 6 is the streamline distribution of the half rotation surface at each span under the 40% gas volume fraction, we can see from the figure, at 0.1 span, the flow separation is more serious, and local position began to appear vortex. At 0.5 span, the vortex is filled with the whole flow field within the guide vane. At 0.9 span, the flow separation is serious, and the out-let of the guide vane begin to appear vortex. As can be seen from figure 4 to figure 6, with the increase of the gas volume fraction, the vortex movement in the guide vane is obviously enhanced, and at the rim of the impeller also began to flow separation.

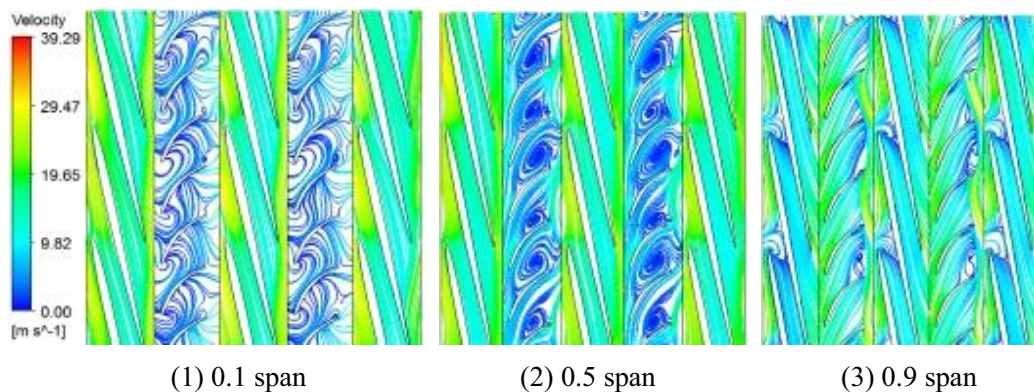


Figure 6. The streamline distribution of the half rotation surface of each span under the conditions of the 40% gas volume fraction

4.2 Turbulence dissipation

Figure 7 is the turbulent dissipation of the half-rotation surface at each span under pure water, from the figure can be seen, from 0.1 span to 0.9 span, the turbulence dissipation of the whole flow field is getting bigger and bigger, but turbulence dissipation is smaller in the impeller and the guide vane, and turbulence dissipation is mainly concentrated in the inlet of the impeller and the exit of the guide vane. Compare figure 4 can be found, the area where the vortex is relatively large is also the region of the turbulence dissipation.

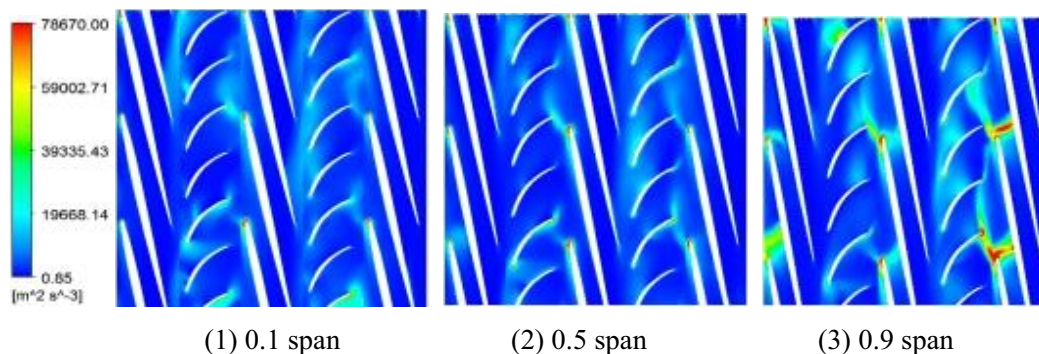


Figure 7. Turbulent dissipation diagram of the half-rotation surface of each span under the pure water condition

Figure 8 is the turbulent dissipation of the half-rotation surface at each span under the 20% gas volume fraction condition, from the figure can be clearly seen, at 0.1 span, the turbulent dissipation region of the impeller inlet area becomes larger than the pure water condition. At 0.5 span, the turbulence dissipation is

relatively uniform, mainly distributed in the impeller and the guide vane junction, and the dissipation between two stage is greater than the dissipation within the stage. At 0.9 span, the turbulent dissipation at the inlet of the impeller is most obvious, mainly because here is more serious separation flow, making energy dissipation faster.

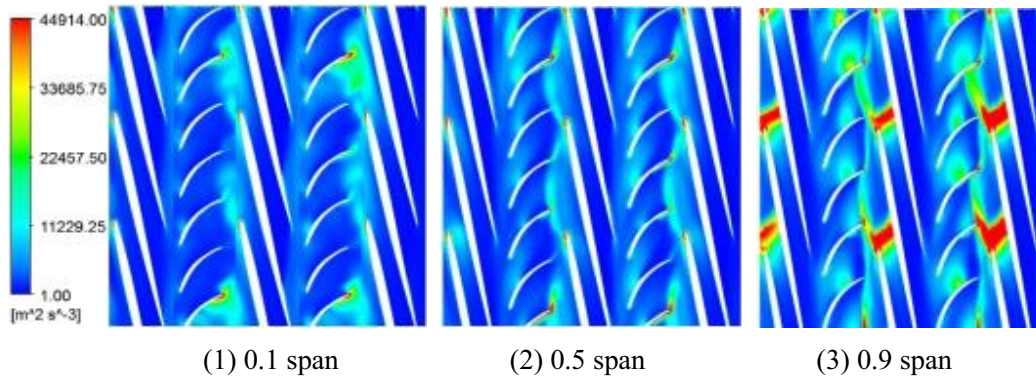


Figure 8. The turbulent dissipation diagram of the half-rotation surface at each span under the 20% gas volume fraction condition

Figure 9 is the turbulent dissipation diagram of the half-rotation surface at each span under the 20% gas volume fraction condition, as can be seen from the figure, at 0.1 span, the turbulence dissipation occurs mainly between the two stages, and which is obvious at the out-let of the guide vane. At 0.5 span, the turbulence dissipation distribution is more uniform, and the overall dissipation is relatively low, mainly concentrated at the out-let of the guide vane and the next stage impeller inlet. At 0.9 span, the turbulence dissipates at the position of the guide vane out-let working face and the inlet of the impeller, from the figure 6 can be found, this part of the area is also mainly the area of the serious flow separation. It can be seen that the effect of flow separation on the turbulence dissipation in the flow path of the multiphase pump is significant, and can be seen from figure7 to figure 9, with the gas volume fraction increases, the region where the maximum turbulent dissipation occurs gradually increases, however, the maximum turbulent dissipation value decreases.

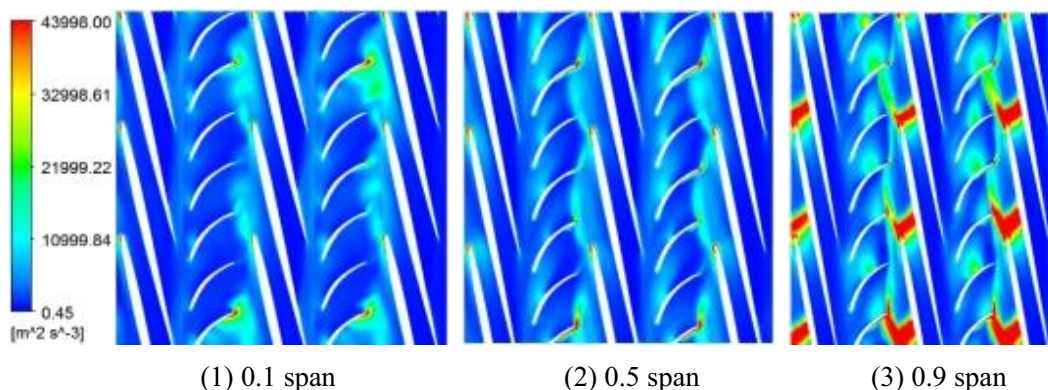


Figure 9. The turbulent dissipation diagram of the half-rotation surface at each span under the 40% gas volume fraction condition

5. Conclusion

Near the impeller hub position, the guide vane inlet has a greater flow separation, covered with the whole guide vane flow field, there is also a backflow within the individual guide vanes, but there is no vortex in the impeller. With the closer to the impeller rim, the number of the vortex is obvious reduced, and the impeller inlet began to appear flow separation. With the increase of the gas volume fraction, the vortex movement in the guide vane is obviously enhanced.

From the impeller hub to the rim, the turbulence dissipation in the flow field is getting bigger and bigger, turbulence dissipation is mainly concentrated in the inlet of the impeller and the out-let of the guide vane. As the gas volume fraction increases, the region where the maximum turbulent dissipation occurs gradually increases, but the maximum turbulent dissipation value decreases.

From the hub to the rim, the vortex within the guide vane is gradually reduced, but the vortex within the impeller is gradually obvious. And with the increase of the gas volume fraction, the flow separation, the backflow and the vortex within the impeller and the guide vane gradually enhanced. It is also found that the effect of flow separation on the turbulence dissipation in the flow field of the multiphase pump is significant, that is, the more serious the area of flow separation, the greater the energy loss.

Acknowledgment

This work was supported by grants from China Postdoctoral Science Foundation (2016M600090), China Postdoctoral Science Foundation (2017T100077), National Natural Science Foundation of China (51279083), Education department key project of Sichuan province of China (17ZA0366), and the Key scientific research fund of Xihua University of China (Z1510417). This work was also supported by the Open Research Subject of Key Laboratory of Fluid and Power Machinery, Ministry of Education (szjj2016-004) and the Economy, Trade and Information Commission of Shenzhen Municipality (201411201645511650).

References

- [1] Ji B, Luo X, Wu Y, et al. *Numerical analysis of unsteady cavitating turbulent flow and shedding horse-shoe vortex structure around a twisted hydrofoil*[J]. International Journal of Multiphase Flow, 2013, 51(5):33-43.
- [2] Zhang Jinya, Cai Shujie, Zhu Hongwu, etc. *Numerical simulation of compressible flow field in three-stage spiral axial flow pump*[J]. Journal of Agricultural Mechanization, 2014, 45 (9): 89-95.
- [3] Yu Zhiyi, Liu Ying. *Analysis of unsteady flow characteristics of gas-liquid two-phase flow in a blade-type mixed pump*[J]. Journal of Agricultural Mechanization, 2013, 44 (5): 66-69.
- [4] Ma Xijin, Bao Chunhui, *Effects of blade number on unsteady flow field in axial-flow oil-gas multiphase pump*[J]. Fluid Mechanics, 2017, 45 (5).
- [5] Zhang W, Yu Z, Zhu B. *Numerical Study of Pressure Fluctuation in a Gas- Liquid Two-Phase Mixed-Flow Pump*[J]. Energies, 2017:634.
- [6] Ma Xijin, Zhang Zhenzhen, Hou Hua. *Effects of axial clearance variation on performance of multi-stage oil-gas multiphase pump*[J]. Fluid Machinery, 2015 (4): 28-32.
- [7] Ma Xi-jin, Jia Weibin, Bao Chunhui. *Flow field analysis of double-ended mechanical seal end face of oil-gas multiphase pump based on fluent*[J]. Hydraulic Pneumatic and Seal, 2015, 35 (12): 16-18.
- [8] Zhang W, Zhu B, Yu Z, et al. *Numerical study of pressure fluctuation in the whole flow passage of a low specific speed mixed-flow pump*[J]. Advances in Mechanical Engineering, 2017, 9(5).
- [9] Gu Shengqin, Li Xinkai, Ma Xijin, etc. *Effects of inlet angle of guide vane on performance of multiphase pump*[C] // National Conference on Hydraulic Machinery and Its System. 2011:

- 52-56.
- [10] Zhang W, Yu Z, Zhu B. *Influence of Tip Clearance on Pressure Fluctuation in Low Specific Speed Mixed-Flow Pump Passage*[J]. *Energies*, 2017, 10(2):148.
 - [11] Xu Y, Tan L, Liu Y, et al. *Pressure fluctuation and flow pattern of a mixed-flow pump with different blade tip clearances under cavitation condition*[J]. *Advances in Mechanical Engineering*,9,4(2017-4-01), 2017.
 - [12] Tan L, Yu Z, Xu Y, et al. *Role of blade rotational angle on energy performance and pressure fluctuation of a mixed-flow pump*[J]. *Proceedings of the Institution of Mechanical Engineers Part A Journal of Power & Energy*, 2017.
 - [13] Li Wei, Ji Leilei, Shi Weidong, etc. *PIV measurement of internal flow field in multi-operating condition of guide vane mixed-flow pump*[J]. *Journal of Agricultural Engineering*, 2016, 32 (24): 82-88.
 - [14] Zhang Jinya, Cai Shujie, Zhu Hongwu. *Visualization test of gas-liquid two-phase flow field in inlet section of vane mixed pump*[J]. *Journal of Mechanical Engineering*, 2015, 51 (18): 184-190.
 - [15] Yang X, Hu C, Hu Y, et al. *Theoretical and experimental study of a synchronal rotary multiphase pump at very high inlet gas volume fractions*[J]. *Applied Thermal Engineering*, 2017, 110:710-719.